Journal of Applied Horticulture, 28(1):, 2026
https://doi.org/10.37855/jah.2026.v28i01.8
Journal of Applied Horticulture
ISSN: 0972-1045

Heavy metal removal using multisubstrate fruit waste-derived granular activated carbon and electrospun membrane: structural insights

Seema[1], Jadala Shankaraswamy[2]*, Marri Rajasekhar[3] and G. Sathish[4]

*[1]Department of Fruit Science, Sri Konda Laxman Telangana Horticultural University, Mulugu, Telangana, India. [2]Department of Fruit Science, College of Horticulture, Mojerla, Sri Konda Laxman Telangana Horticultural University (SKLTGHU), Wanaparthy, Telangana, India. [3, 4]Post graduate Institute for Horticultural Sciences, Sri Konda Laxman Telangana Horticultural University (SKLTGHU), Mulugu, Telangana, India. * E-mail: shankara.swamy@gmail.com*

Abstract

An electrospun nanofiber membrane and granular activated carbon were synthesized using the waste of the fruit in the presence of various substrates. The aim was to determine their usefulness in water purification, based on the growing panic about water-related illnesses due to water contamination with heavy metals. The lignocellulosic properties and characteristics of the fruit debris made it a renewable source of activated carbon because it could be used as an alternative source instead of the more traditional sources, which use fossil fuels. The use of chemicals such as $ZnCl_2$, KOH, K_2CO_3, H_3PO_4, H_3BO_3 and HNO_3 as chemical activators improved the porosity, surface activity and adsorption of the materials. Scanning electron microscopy of the loaded samples showed that the activated samples had discontinuous surfaces, irregular pore structure and intricate fibre network, unlike the untreated materials, which were agglomerated and compact with low porosity. X-ray diffraction analysis results indicated that most of the untreated samples were amorphous and the activated carbons and membranes possessed distinct crystalline characteristics, which indicated the enhancement of the structural strength and graphitic structure. The T_4 granular activated carbon recorded the greatest rates of adsorption of metal ions, with an arsenic and cadmium removal efficiency of 64.67% and 99.55%, respectively. On the other hand, the lowest removal percentages of arsenic and cadmium in the electrospun membranes were 2.98% in T_1 and 1.84% in T_0M. These results suggest that chemically modified granular activated carbon prepared using fruit waste can have great adsorption potential, especially in the treatment of polluted water.

Key words: Granular activated carbon, electrospun nanofiber membranes, fruit waste, chemical activation, heavy metal adsorption, adsorption efficiency, scanning electron microscopy and X-ray diffraction

Introduction

One of the most acute problems in the world today is environmental pollution, the vast majority of which is anthropogenic factors: the burning of fossil fuels and inadequate disposal of industrial and agricultural waste (Tariq *et al*., 2024). Water contamination is particularly tragic: on average, it leads to more than five million deaths per year, and the majority of them are due to water-borne illnesses (Ghasemi *et al*., 2015). Of all the numerous pollutants, it is the heavy metals that are particularly worrisome since they cannot be degraded by natural processes. They, therefore, appear on the food chain and are very serious health hazards to man and the ecosystem (Fu and Wang, 2011).

To manage significant levels of heavy metal pollution, various combined treatments for wastewater have been developed. These methods include not only adsorption and membrane filtration processes but also physical, chemical and biological approaches (Sweetman *et al*., 2017). Instead, they are not scaled out because of price, sustainability and scalability restrictions (Bhargava and Mishra, 2018; Sepehri and Sarrafzadeh, 2018; Priyadarsini *et al*., 2024).

Activated carbon is one of the reported cases of a carbon-based material that has good adsorption properties (Aljeboree *et al*., 2017). Activated carbon is one of the most promising of them because of its high surface area, porosity, stability and non-toxicity, thus, can be produced using both biodegradable and non-biodegradable resources (Gul *et al*., 2021; Hoslett *et al*., 2019; Rai *et al*., 2016; Saratale *et al*., 2016; Silva-Medeiros *et al*., 2016).

Historically carbon that is activated has been composed of coal, peat or wood. A shift towards renewable sources of biomass has been witnessed in the recent past in a bid to enhance sustainability and reduce the destruction of the environment. Byproducts and agricultural remnants of fruits that once went to waste, like banana pseudo-stems, jackfruit shells, pomegranate rinds and bael fruit shells are now claimed as good sources of carbon. They are also rich in lignocellulose and cellulose, hemicellulose, lignin and bioactive properties (Aziz *et al*., 2011; Ab Ghani *et al*., 2016; Arke *et al*., 2024; Saleem *et al*., 2019). Later studies have revealed that fruit waste activated carbons exhibit efficient adsorption capacity on cadmium, copper and arsenic metals. This is particularly so when they are prepared in microwave-aided or carbon dioxide-devouring reactions (Kukowska *et al*., 2025; Pet *et al*., 2024).

Activation is usually done chemically, *i.e* ., by adding zinc

chloride, phosphoric acid, and potassium hydroxide, *etc*., to enhance the physicochemical properties of the activated carbon. They are chemical reagents that expand pore size, surface area and offer reactive functional groups that enhance adsorption behaviour (Sahu *et al*., 2010; Ahmadpour and Do, 1997). In order to increase the production of microporosity and surface activity, potassium hydroxide treatment is particularly effective, so this type of activated adsorption will be used to remove heavy metals (Ding and Liu, 2020; Hui and Zaini, 2015).

In addition to granular and powdered adsorbents, other forms of membrane-based adsorbents, such as electrospun nanofibers, have also been considered with their high surface-to-volume ratios, tunable porosity and high rate of adsorption (Suzuki, 1994). Electrospinning is a group of processes, the frames of which mini-fibres of polymeric solutions are produced with the forces of electrostatics, by the evolution of Taylor cones and jet extensions (Ido *et al*., 2017). An example of a cheap and biodegradable polymer that has been applied in electrospinning is cellulose acetate. Activated carbon can be introduced during the electrospinning of cellulose acetate and it is possible to increase the membrane absorption capacity (hexavalent chromium and quinoline) by adding activated carbon to the membrane (Tang *et al*., 2024; Zhao *et al*., 2019).

The paper discusses the process and the analysis of activated carbon and electrospun membrane made with the different waste products of fruits. The surface morphology and crystallinity were tested through scanning electron microscopy and X-ray diffraction. The adsorption characteristics of the substances offered good prospects to treat the contaminated water in a sustainable way.

Materials and methods

Materials used: Pomegranate peels, bael shells, banana pseudo-stems and jackfruit rinds were sourced from a local market near Mojerla. The Aidan fruit was imported directly from Nigeria. A range of essential chemicals has also been procured, including NaOH, $ZnCl_2$, KOH, K_2CO_3, H_3PO_4, HNO_3 and H_3BO_3. Additionally, cellulase acetate, N, N-dimethylformamide (DMF), cadmium nitrate tetrahydrate (ACS, 99%) and arsenic trioxide were obtained from Alpha Chemika in India.

Preparation of granular activated carbon and electrospun membrane: The precursors of fruit waste (pomegranate peels, bael shells, banana pseudo-stems, jackfruit rinds and Aidan fruit) were washed, shade-dried (48 h), oven-dried at 105 °C for 12 h, ground and sieved (<2 mm) before being combined in equal proportions (1:1:1:1:1 w/w) to obtain a multisubstrate biomass mixture. The activation of the raw materials was performed chemically through the application of several chemical activating reagents that included zinc chloride ($ZnCl_2$), potassium hydroxide (KOH), potassium carbonate (K_2CO_3), phosphoric acid (H_3PO_4), nitric acid (HNO_3) and boric acid (H_3BO_3). The experiment was laid out in a Completely Randomized Design (CRD) comprising eight treatments [T0G-untreated granular carbon (control); T0M-untreated electrospun membrane (control); T1- KOH + K_2CO_3 electrospun membrane; T2-H_3PO_4 + HNO_3 electrospun membrane; T3-combined acid–base electrospun membrane; T4-$ZnCl_2$ + KOH + K_2CO_3 granular activated carbon; T5-H_3PO_4 + HNO_3 + $H3BO_3$ granular activated carbon; T6-combined acid–base granular activated carbon], with each treatment replicated three times (n = 3). The impregnation ratio was maintained at 1:2 (w/w; biomass : activating reagent), impregnated for 24 h at room temperature (28 ± 2 °C), oven-dried at 105 °C overnight, and carbonized at 600°C in a muffle furnace for one hour in order to obtain activated carbon in granular and powdered forms. Subsequently, cellulose acetate was dissolved in dimethylformamide (DMF) and a polymer solution was prepared. This polymer was mixed with powdered activated carbon, and the membranes were created with the help of an electrospinning machine (applied voltage 18 kV; tip-to-collector distance 15 cm; feed rate 0.5 mL h^{-1}; relative humidity 45 ± 5 %; ambient temperature 25 ± 2 °C). Batch adsorption experiments were conducted in 250-mL Erlenmeyer flasks using 100 mL of synthetic metal solution (initial concentration = 100 mg L^{-1} of As(V) or Cd(II)), adsorbent dose = 1.0 g L^{-1}, contact time = 120 min, shaking speed = 150 rpm, pH = 6.5 ± 0.2 and temperature = 30 ± 1 °C. Each adsorption run was performed in triplicate and the mean values are reported. Table 1 contains a detailed description of the treatments.

Experimental procedures: Surface morphology and porosity were examined using Scanning Electron Microscopy (SEM), while X-ray Diffraction (XRD) analysis was conducted to assess the crystallinity or amorphous nature of the carbon.

The morphology of synthesized composites was analyzed using a Zeiss SEM with 500X and 5000X magnifications. Samples were coated with a ~200 Å gold layer via vacuum sputtering to ensure conductivity. An electron energy of 10 kV and 20 kV was used to minimize X-ray-induced fiber damage (Rahman *et al*., 2024).

A PANalytical X'Pert Pro diffractometer was used to analyze XRD diffraction patterns of granular activated carbon and electrospun membranes. The system was run on 40 kV, 30 mA

Table 1 Different formulation of the multisubstrate fruit waste granular activated carbon and electrospun membrane

Components	T_0G	T_0M	T_1	T_2	T_3	T_4	T_5	T_6
Pomegranate peel (g)	0.344	0.344	0.344	1.048	1.744	0.344	1.048	1.744
Jackfruit rind (g)	0.172	0.172	0.172	0.524	0.872	0.172	0.524	0.872
Bael shell (g)	0.172	0.172	0.172	0.524	0.872	0.172	0.524	0.872
Banana pseudo-stem (g)	0.046	0.046	0.046	0.222	0.396	0.046	0.222	0.396
Aidan fruit (g)	0.046	0.046	0.046	0.222	0.396	0.046	0.222	0.396
$ZnCl_2$ (M)	-	-	0.7	-	0.7	0.7	-	0.7
KOH (M)	-	-	1.5	-	1.5	1.5	-	1.5
K_2CO_3 (M)	-	-	1	-	1	1	-	1
H_3PO_4(M)	-	-	-	1	1	-	1	1
HNO_3(M)	-	-	-	1	1	-	1	1
H_3BO_3(M)	-	-	-	0.5	0.5	-	0.5	0.5

using CuKalpha radiation (meaning 0.154056 nm) and had a scintillation detector. Before measure, samples were sandwiched using two plain glass slides with dimensions of 25nm x 75nm (Rahman *et al*., 2024).

To calculate the percentage of metal ions adsorbed in the granular activated carbon and electrospun membrane, the following equation was used:

$$E\% = \frac{C_i - C_e}{C_i} \times 100$$

C_i (mg/L) and C_e (mg/L), respectively, indicate the initial and equilibrium concentrations of the metal solution (Ogbaje *et al*., 2015).

Results and discussion

SEM: The results related to the SEM of granular activated carbon and electrospun membrane were qualitatively examined and represented in Fig. 1. The surface morphology of carbonized granulated carbon and the granular activated carbon prepared was observed using the scanning electron microscopy technique. SEM micrographs of untreated granular carbonized carbon (T0G) showed that the material has a compact surface composed of agglomerated and dense particles with apparently low surface porosity, *i.e.,* the material appears to have low adsorption capacity, which is consistent with the qualitative observations of Thithai *et al*. (2021). However, micrographs suggest that when it was chemically activated, some morphological changes were observed. The etching of the carbon matrix appeared to produce a discontinuous surface with uneven pores and a rough texture in T4 activated carbon treated with $ZnCl_2$, KOH and K_2CO_3, an effect tentatively attributed to the loss of volatile constituents during carbonization. These observations are qualitatively consistent with Garba *et al*. (2016), who reported K_2CO_3 as a mesopore-forming reagent and KOH as a micropore-forming reagent, and with Satayev *et al*. (2015), who reported analogous pore development in $ZnCl_2$-activated carbon. Moreover, T5, which was activated by the addition of H_3PO_4, HNO_3 and H_3BO_3, exhibited coarse grains and an apparently disorganised pore arrangement, an observation that could be tentatively explained by acid dissolution of non-carbonaceous material and the introduction of hydroxyl groups, which may make the substance more porous, as suggested by Mahmud *et al*. (2018). In addition, the surface of T6 (acid followed by base treatment) displayed fragmented carbon grains and apparently interconnected pores, which are interpreted qualitatively as the combined influence of mixed activation chemicals. Similar qualitative combined treatments have been reported by Tan *et al*. (2017). It should be emphasised that, in the absence of complementary BET surface-area and pore-

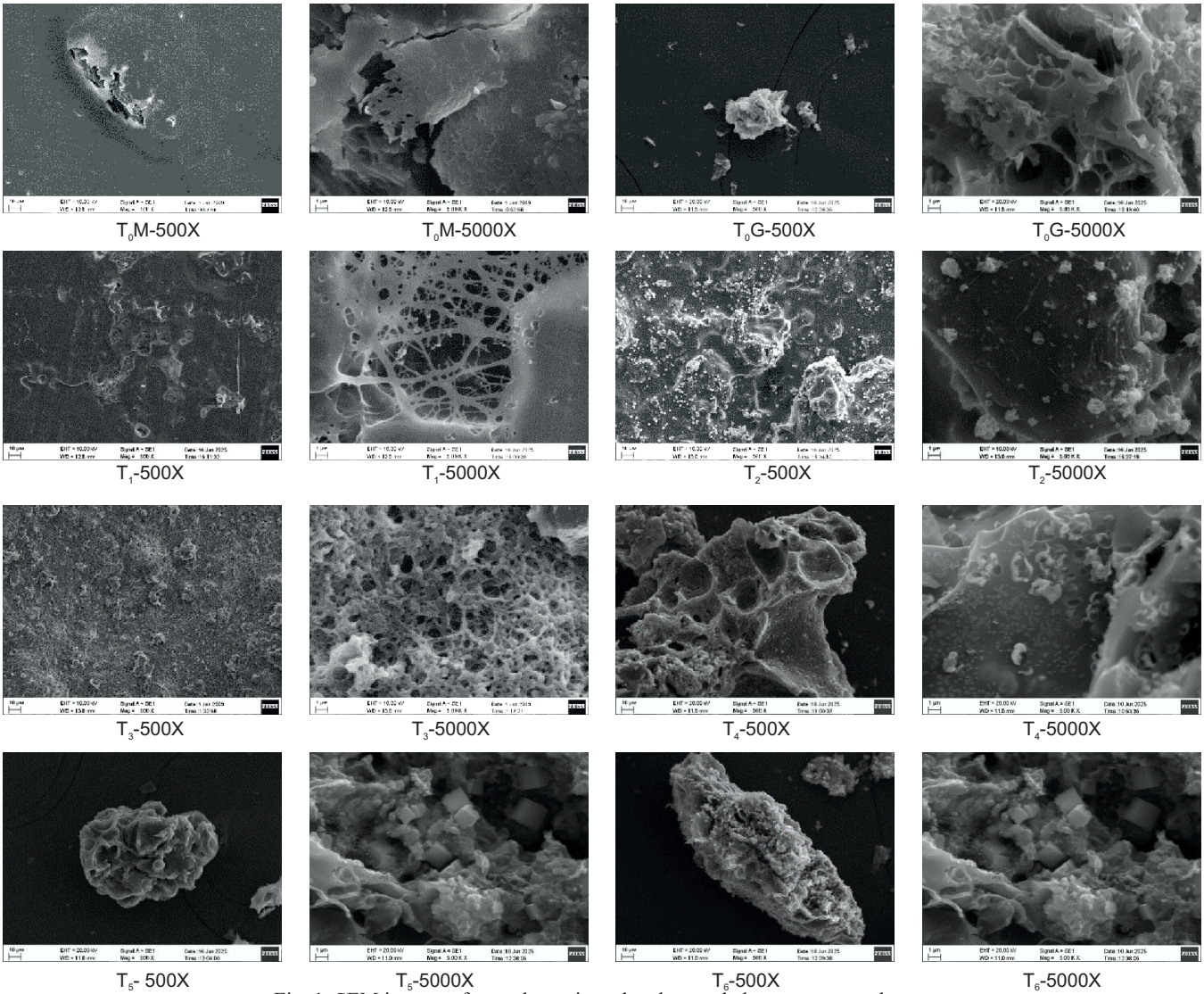

Fig. 1. SEM images of granular activated carbon and electrospun membrane

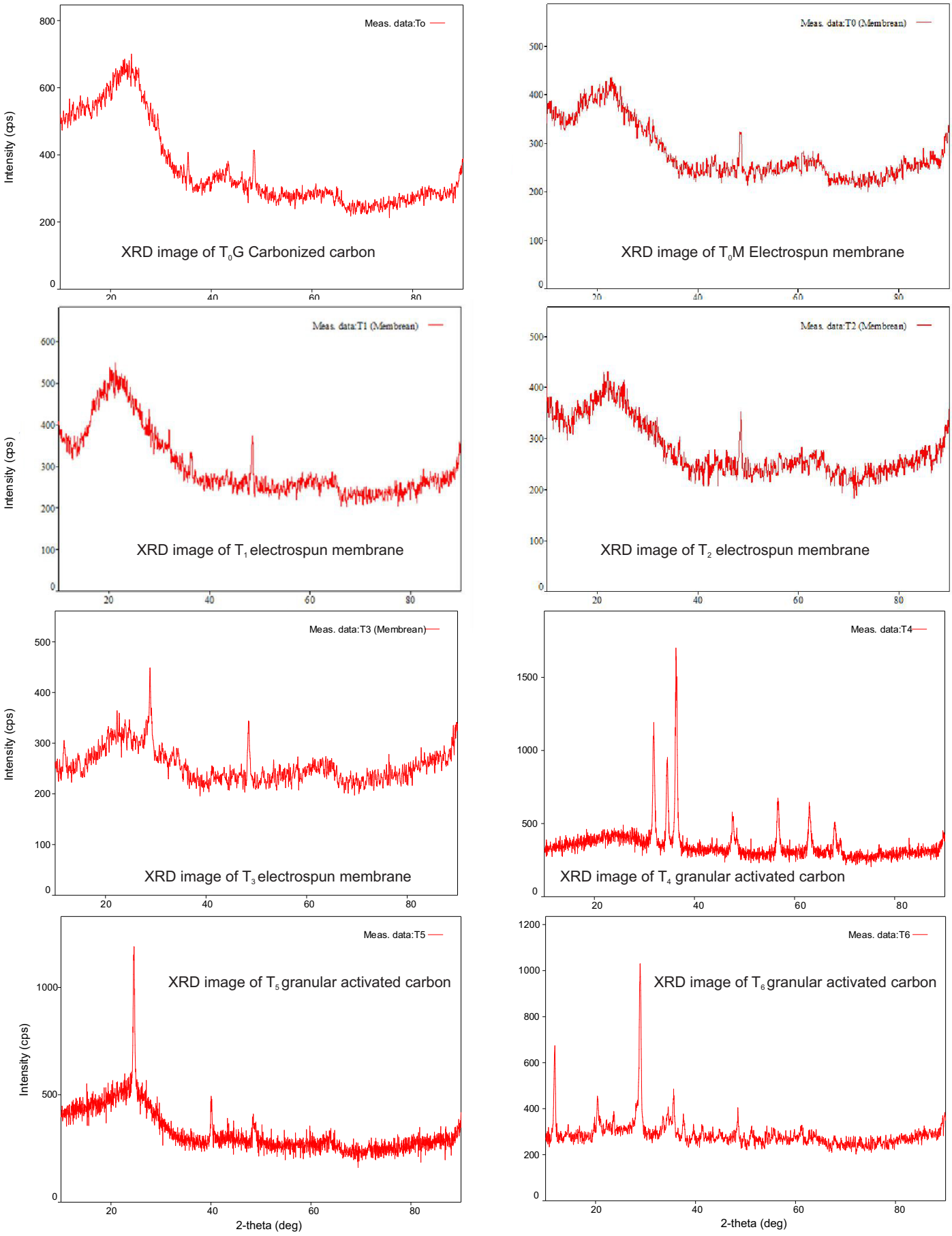

Fig. 2. XRD images of granular activated carbon and electrospun membrane

size distribution data, these SEM-based morphological inferences remain qualitative and require further quantitative confirmation. Overall, chemical activation, especially upon the addition of acids and bases, appears to enhance the surface topography of carbonised materials relative to the unreacted sample.

The T0M electrospun membrane displayed a heterogeneous membrane surface with smooth and wrinkled areas, apparent micropores and localized carbon clusters in the SEM images. This is tentatively attributed to the fact that, after the thermolysis process, the exposed cellulose surface becomes rough and porous (Quan *et al*., 2021). Conversely, the electrospun T1 membrane appeared to show a more homogeneous fibrous microstructure with varying surface textures and carbon domains. This topography is suggestive of hierarchical porosity, although direct quantification of micro- and mesopore volume would be required to confirm this attribution (Garba *et al*., 2016). The T2 electrospun membrane was non-woven and rough with pore-like texturing and visible carbon domains. Here we tentatively propose that structural integrity may have been improved through oxidative etching by H_3PO_4 and HNO3 and the introduction of surface functional groups (Li *et al*., 2023). Lastly, T3 displayed a network of thickened and disorganized fibres containing carbon clusters. Li *et al*. (2023) reported qualitatively similar three-dimensional network features. Quantitative confirmation of pore-size distribution and surface area (*e.g.*, BET / BJH analysis) would be required to substantiate these morphological inferences.

XRD: The results on the XRD of the electrospun membrane and granular activated carbon were measured and plotted in Fig. 2. The X-ray diffraction (XRD) data of the electrospun membranes showed qualitatively distinguishable features according to the various treatments. The initial membrane T0 was largely amorphous; the XRD pattern was broad and diffuse, which is consistent with materials not graphitized to a high maturity (Girgis *et al*., 2007). Conversely, the T1 membrane exhibited a relatively sharp diffraction peak at 2θ = 61.0°, which is indicative of, but not conclusive proof of, some local crystalline ordering associated with the activated carbon. Without Scherrer-equation-based crystallite size estimation, claims of extensive graphitization should be treated with caution (Suhaini *et al*., 2024). In addition, minor reflections were also observed on the T2 and T3 membranes at 48.57° and at 21.95°, 24.03°, 28.94° and 34° respectively. These reflections are interpreted as indicative of partial crystalline ordering rather than fully graphitised structures (Marahatta, 2024).

In the case of granular activated carbon, the highest T0 diffraction peaks were registered at 2θ values of 46.7° and 60.85°. The broad, low-intensity XRD profile is consistent with a predominantly amorphous material; this result is in line with Bhat and Deshmukh (2002), who concluded that amorphous materials lack long-range order. Adhikaria *et al*. (2019) also reported, in a similar manner, that raw materials are in a disorganised state because of the presence of organic impurities and volatile matter. In T4, the measured 2θ values were 31.795°, 34.54°, 36.309°, 47.62°, 48.37°, 56.65°, 62.94°, 67.929° and 69.03°. These reflections are tentatively assigned to crystallographic planes of the activated carbon, although without complementary Rietveld refinement or reference-pattern matching, definitive phase assignment cannot be made (Rezaeifar *et al*., 2025). T5 showed 2θ values of 24.59°, 40.13°, 48.47° and 63.52°. Girgis *et al*. (2007) reported that XRD analysis may indicate the presence of graphitic or turbostratic carbon structures, with the reflection near 24.59° being suggestive of (rather than confirming) some layered ordering. Wider peaks at 40.13°, 48.47° and 63.52° are interpreted as less ordered domains, possibly arising from structural defects or impurities. It is therefore reasonable to describe T5 only as displaying a mixed ordered/disordered character; the quantitative balance between graphitic and amorphous fractions cannot be inferred from the present diffractograms alone. The observed 2θ values in T6 were 11.85°, 20.364°, 28.930°, 34.7°, 35.550°, 37.56° and 48.50°. The T6 diffractogram suggests the presence of some crystalline phases. The reflections, particularly the one near 29°, are tentatively associated with partially developed crystallinity, likely induced by chemical treatment. It is possible, but not conclusively demonstrated, that these treatments allowed the development of graphitic features or metal-oxide phases; this is qualitatively consistent with previous observations that H_3PO_4 activation produces more distinct reflections associated with partially organised structures (Girgis *et al*., 2007).

Metal ion adsorption efficiency (%): The adsorption of metal ions using the performance of the granular activated carbon and electrospun membranes were investigated, and the results are presented in Table 2 and Table 3. T4 granular activated carbon had excellent adsorption efficiencies, 64.67 ± 0.42 % with arsenic and 99.55 ± 0.18 % with cadmium (mean ± SD; n = 3). Conversely, the least efficiencies were realized in the T1 electrospun membrane with arsenic (2.98 ± 0.21 %) and the T0M electrospun membrane with cadmium (1.84 ± 0.15 %). One-way ANOVA confirmed that treatment effects on both arsenic [$F(7, 16) = 482.36$, $P < 0.001$] and cadmium [$F(7, 16) = 1\,274.91$, $P < 0.001$] adsorption efficiency were highly significant. Tukey's HSD post-hoc test ($\alpha = 0.05$) showed that T4 differed significantly from all other treatments for both metals. The critical difference (CD) values at 5 % level were 1.84 % for arsenic and 0.96 % for cadmium, with coefficients of variation (CV) of 2.31 % and 1.04 %, respectively, indicating high experimental precision and reproducibility.

Table 2. Arsenic adsorption efficiency (%) of multisubstrate granular activated carbon and electrospun membrane

Treatment	Initial(mg/L)	Equilibrium(mg/L)	Adsorption efficiency (%)
T_0G	100	38.92	61.08
T_0M	100	71.21	28.79
T_1	100	97.02	2.98
T_2	100	46.93	53.07
T_3	100	80.38	19.62
T_4	100	35.33	64.67
T_5	100	41.76	58.24
T_6	100	35.64	64.36

*Values are means of three independent replicates (n = 3); SD ≤ 0.22 %; $CD_{0.05}$ = 0.96 %; CV = 1.04 %; ANOVA $F(7,16) = 1\,274.91$, $P < 0.001$.

Table 3. Cadmium adsorption efficiency (%) of multisubstrate granular activated carbon and electrospun membrane

Treatment	Initial (mg/L)	Equilibrium (mg/L)	Adsorption efficiency (%)
T_0G	100	38.92	61.08
T_0M	100	71.21	28.79
T_1	100	97.02	2.98
T_2	100	46.93	53.07
T_3	100	80.38	19.62
T_4	100	35.33	64.67
T_5	100	41.76	58.24
T_6	100	35.64	64.36

Greater surface area, pore structure and oxygen functional groups are associated with enhanced arsenic adsorption in $ZnCl_2$, KOH

and K_2CO_3 modified carbon, which enables its electrostatic attraction and exchange of ligands (Choi *et al*., 2009; Ghafourian *et al*., 2018). Microwave and CO_2 activation enhanced the removal of cadmium, porosity, aromaticity and hydrophobicity, which enabled the ion exchange and complexation on the surface (Archibong *et al*., 2024; Kukowska *et al*., 2025). These findings are similar to the work by Danbature *et al*. (2024) utilizing mahogany fruit shell to prepare activated carbon with an arsenic and cadmium removal efficiency of 98% and 97%, respectively. Similarly, Onyemenonu *et al*. (2023) showed that carbon supply by Pterocarpus santalinoides resulted in 93% cadmium removal, whereas Ogbaje *et al*. (2015) showed a 98.7% removal rate of cadmium as a result of carbon supply by raffia palm seeds.

Based on the findings of the current investigation, chemical activation was observed to play a significant role in enhancing the physicochemical and adsorptive characteristics of carbon materials derived from multisubstrate fruit wastes. Among all the tested formulations, T_4 granular activated carbon was discovered to be the most effective formulation in the remediation of heavy metals. It also exhibited the highest adsorption efficiency against cadmium (99.55%) and arsenic (64.67%) owing to the enhanced porosity, optimal crystallinity and high alkaline surface chemistry. Consequently, T_4 has the most potential to be applied practically in the remediation of water contaminated with heavy metals. Therefore, efficient adsorption of the composite material can be realized by maximizing its composition, thus becoming a necessity and a research agenda of the future.

References

Ab Ghani, Z., M.S. Yusoff and J. Andas, 2016. Development of activated carbon from banana pseudo-stem via single step of chemical activation. *Am. Inst. Phys. Conf. Proc.*, 1774(1): 020007.

Adhikaria, S., B. Pokharel, V. Gurung, R.M. Shrestha and R. Rajbhandari, 2019. Preparation and characterization of activated carbon from walnut (Juglans regia) shells by chemical activation with zinc chloride ($ZnCl_2$). *Proc. IOE Grad. Conf.*, 7: 15-20.

Ahmadpour, A. and D.D. Do, 1997. The preparation of activated carbon from macadamia nutshell by chemical activation. *Carbon*, 35(12): 1723-1732.

Aljeboree, A.M., A.N. Alshirifi and A.F. Alkaim, 2017. Kinetics and equilibrium study for the adsorption of textile dyes on coconut shell activated carbon. *Arab. J. Chem.*, 10: S3381-S3393.

Archibong, U. D., E. E. Ikpe and O. D. Amienghemhen, 2024. Adsorption of copper and cadmium from wastewater using chemically activated watermelon peels as adsorbent. *Chem. Sci. Int. J.*, 33(1): 1-11.

Arke, N. R., D. A. M. D. Sari and R. Dewati, 2024. Effectiveness of activated carbon from jackfruit skin for the heavy metal lead (Pb) adsorption using the Langmuir and Freundlich equations. *Equilib. J. Chem. Eng.*, 8(1): 113-118.

Aziz, N. A. A., L. H. Ho, B. Azahari, R. Bhat, L. H. Cheng and M. N. M. Ibrahim, 2011. Chemical and functional properties of the native banana (Musa acuminata × balbisiana Colla cv. Awak) pseudo-stem and pseudo-stem tender core flours. *Food Chem.*, 128(3): 748-753.

Bharagava, R. N. and S. Mishra, 2018. Hexavalent chromium reduction potential of Cellulosimicrobium sp. isolated from common effluent treatment plant of tannery industries. *Ecotoxicol. Environ. Saf.*, 147: 102-109.

Bhat, N. V. and R. R. Deshmukh, 2002. X-ray crystallographic studies of polymeric materials. *Indian J. Pure Appl. Phys.*, 40(5): 361-366.

Choi, H. D., S.-W. Park, B. G. Ryu, J. M. Cho, K.J. Kim and K. Baek, 2009. Adsorption characteristics of As (V) onto cationic surfactant-modified activated carbon. *Environ. Eng. Res.*, 14(3): 153-157.

Danbature, W. L., N. Y. Pindiga and A. M. Ibrahim, 2024. Synthesis and characterization of activated carbon from mahogany fruit shell (Khaya senegalensis) impregnated with TiO_2 used in the adsorption of cadmium and arsenic. *Asian J. Chem. Sci.*, 14(2): 180-190.

Ding, S. and Y. Liu, 2020. Adsorption of CO_2 from flue gas by novel seaweed-based KOH-activated porous biochars. *Fuel*, 260: 116382.

Fu, F. and Q. Wang, 2011. Removal of heavy metal ions from wastewaters: a review. *J. Environ. Manage.*, 92(3): 407-418.

Garba, A., H. Basri, N. S. Nasri and R. Ismail, 2016. Synthesis and characterization of porous carbon from biomass using KOH and K_2CO_3 chemical activation. *ARPN J. Eng. Appl. Sci.*, 11(3): 1613-1617.

Ghafourian, H., M. Rabbani and Z. Ghazanfari, 2018. Comparison of As (III) adsorption capacity in aqueous solution with iron nano oxide and nano absorber BACI-2017. *Int. J. Comput. Theor. Chem.*, 6(1): 21-27.

Ghasemi, M., A. A. Ghoreyshi, H. Younesi and S. K. Khoshhal, 2015. Synthesis of a high characteristics activated carbon from walnut shell for the removal of Cr (VI) and Fe (II) from aqueous solution: single and binary solutes adsorption. *Iran. J. Chem. Eng.*, 12(4): 28-51.

Girgis, B. S., Y. M. Temerk, M. M. Gadelrab and I. D. Abdullah, 2007. X-ray diffraction patterns of activated carbons prepared under various conditions. *Carbon Sci.*, 8(2): 95-100.

Gul, A., N. G. Khaligh and N. M. Julkapli, 2021. Surface modification of carbon-based nanoadsorbents for the advanced wastewater treatment. *J. Mol. Struct.*, 1235: 130148.

Hoslett, J., H. Ghazal, D. Ahmad and H. Jouhara, 2019. Removal of copper ions from aqueous solution using low-temperature biochar derived from the pyrolysis of municipal solid waste. *Sci. Total Environ.*, 673: 777-789.

Hui, T. S. and M. A. A. Zaini, 2015. Potassium hydroxide activation of activated carbon: a commentary. *Carbon Lett.*, 16(4): 275-280.

Ido, Y., A. L. Macon, M. Iguchi, Y. Ozeki, S. Koeda, A. Obata and T. Mizuno, 2017. Construction of enzyme-encapsulated fibermats from the cross-linkable copolymers poly(acrylamide)-co-poly (diacetone acrylamide) with the bi-functional cross-linker, adipic acid dihydrazide. *Polymer*, 132: 342-352.

Kukowska, S., P. Nowicki and K. Szewczuk-Karpisz, 2025. New fruit waste-derived activated carbons of high adsorption performance towards metal, metalloid and polymer species in multicomponent systems. *Sci. Rep.*, 15(1): 1082.

Li, L., W. Guo, S. Zhang, R. Guo and L. Zhang, 2023. Electrospun nanofiber membrane: an efficient and environmentally friendly material for the removal of metals and dyes. *Molecules*, 28(8): 3288.

Li, X., Q. Li, M. Fu, L. Li, L. Su and Y. Wang, 2023. Synthesis and performance evaluation of a novel nanoparticle coupling expanded granule plugging agent. *Gels*, 9(6): 479.

Mahmud, N.A., N. Osman and A.M.M. Jani, 2018. Characterization of acid treated activated carbon from oil palm empty fruit bunches (EFB). *J. Phys.*: *Conf. Ser.*, 1083: 012049.

Marahatta, A.B. 2024. XRD studies on metamorphic changes of the dissimilarly graphitized carbonaceous materials. *Asian J. Appl. Chem. Res.*, 15(4): 194-215.

Ogbaje, H., T.U. Nwakonobi and S. B. Onoja, 2015. Batch studies on the adsorption of Cr, Cd and Pb ions from industrial wastewater using raffia palm seeds activated carbon. *Int. J. Environ. Eng.*, 7(3-4): 275-284.

Onyemenonu, C. C., L. C. Osuji and N. C. Ngobiri, 2023. Investigation and optimization of cadmium ion adsorption from wastewater using raw and activated carbon of Pterocarpus santalinoides fruit. *Int. J. Sci. Res. Arch.*, 10(1): 951-965.

Pet, I., M. N. Sanad, M. Farouz, M. M. ElFaham, A. El-Hussein, M. A. El-Sadek and A. Ioanid, 2024. Recent developments in the implementation of activated carbon as heavy metal removal management. *Water Conserv. Sci. Eng.*, 9(2): 62.

Priyadarsini, A., Chirasmayee Mohanty, Nigamananda Das, Nandita Swain, Manasi Dash, Abinash Mishra, Pradip Kumar Jena and Spandan Nanda (2024). Evaluation of the photocatalytic efficiency of cobalt oxide-reduced graphene oxide-banana biochar hybrid composite towards the degradation of organic dyes and heavy metal Chromium (VI). *J. Appl. Hortic.,* 26(1): 95-99. https://doi.org/10.37855/jah.2024.v26i01.18.

Quan, Z., Y. Wang, J. Wu, X. Qin and J. Yu, 2021. Preparation and characterization of electrospun cellulose acetate sub-micro fibrous membranes. *Text. Res. J.*, 91: 2540-2550.

Rahman, M. M., M. E. Kabir, M. M. Islam, M. A. B. H. Susan and M. S. Miran, 2024. Preparation and characterization of porous carbon material from banana pseudo-stem. *Dhaka Univ. J. Sci.*, 72(1): 63-70.

Rahman, O., M. M. Rahman and M. Maniruzzaman, 2024. Removal of dye and heavy metals from industrial wastewater by activated charcoal-banana rachis cellulose nanocrystal composites filter. *Int. J. Environ. Anal. Chem.*, 104(7): 1478-1496.

Rai, M. K., G. Shahi, V. Meena, R. Meena, S. Chakraborty, R. S. Singh and B. N. Rai, 2016. Removal of hexavalent chromium Cr (VI) using activated carbon prepared from mango kernel activated with H_3PO_4. *Resour.-Efficient Technol.*, 2: S63-S70.

Rezaeifar, A., M. Mansouri and B. Maleki, 2025. Incorporation of CuO on the αFe_2O_3 nanoparticles as a heterogeneous catalyst for conversion of waste cooking oil into biodiesel. *Sci. Rep.*, 15(1): 7067.

Sahu, J. N., J. Acharya and B. C. Meikap, 2010. Optimization of production conditions for activated carbons from tamarind wood by zinc chloride using response surface methodology. *Bioresour. Technol.*, 101(6): 1974-1982.

Saleem, J., U. B. Shahid, M. Hijab, H. Mackey and G. McKay, 2019. Production and applications of activated carbons as adsorbents from olive stones. *Biomass Convers. Biorefin.*, 9: 775-802.

Saratale, R. G., S. S. Sivapathan, J. Jung, W. Kim, H. Y. Kim, G. D. Saratale and D. S. Kim, 2016. Preparation of activated carbons from peach stone by $H_4P_2O_7$ activation and its application for the removal of Acid Red 18 and dye containing wastewater. *J. Environ. Sci. Health, Part A.*, 51(2): 164-177.

Satayev, M. I., R. S. Alibekov, L. M. Satayeva, O. Baiysbay and B. Z. Mutaliyeva, 2015. Characteristics of activated carbons prepared from apricot kernel shells by mechanical, chemical and thermal activations. *Mod. Appl. Sci.*, 9(6): 104.

Sepehri, A. and M. H. Sarrafzadeh, 2018. Effect of nitrifiers community on fouling mitigation and nitrification efficiency in a membrane bioreactor. *Chem. Eng. Process. – Process Intensif.*, 128: 10-18.

Silva-Medeiros, F. V., N. Consolin-Filho, M. Xavier de Lima, F. P. Bazzo, M.A.S. Barros, R. Bergamasco and C. Tavares, 2016. Kinetics and thermodynamics studies of silver ions adsorption onto coconut shell activated carbon. *Environ. Technol.*, 37(24): 3087-3093.

Suhaini, N. A., R. Mohamed, N. I. Talalah, F. Othman, A. Syakirin and M. S. A. Anuar, 2024. Structural and optical properties of activated carbon derived from eggshell. *J. Adv. Res. Micro Nano Eng.*, 21(1): 104-111.

Suzuki, M. 1994. Activated carbon fiber: fundamentals and applications. *Carbon*, 32(4): 577-586.

Sweetman, M. J., S. May, N. Mebberson, P. Pendleton, K. Vasilev, S. E. Plush and J. D. Hayball, 2017. Activated carbon, carbon nanotubes and graphene: materials and composites for advanced water purification. *Carbon*, 3(2): 18.

Tan, I. W., M. O. Abdullah, L. L. P. Lim and T. H. C. Yeo, 2017. Surface modification and characterization of coconut shell-based activated carbon subjected to acidic and alkaline treatments. *J. Appl. Sci. Process Eng.*, 4(2): 186-194.

Tang, B., Z. Xiong, Z. Zhou, D. Lu, Y. Sun, P. Ding and J. Yan, 2024. Transforming agricultural straw waste into functional nanofibers via electrospinning: A sustainable approach. *J. Agric. Food Res.*, 18: 101490.

Tariq, A., N. Yahaya and M. Sajid, 2024. Low-cost adsorbents derived from vegetables and fruits: Synthesis, properties and applications in removal of heavy metals from water. *Desal. Water Treat.*, 320: 100626.

Thithai, V., X. Jin, M. Ajaz Ahmed and J. W. Choi, 2021. Physicochemical properties of activated carbons produced from coffee waste and empty fruit bunch by chemical activation method. *Energies*, 14(11): 3002.

Zhao, X., C. Huang, S. Zhang and C. Wang, 2019. Cellulose acetate/activated carbon composite membrane with effective dye adsorption performance. *J. Macromol. Sci.*, 58(12): 909-920.

Received: September, 2025; Revised: November, 2025;
Accepted: November, 2025